Toxicologic Pathology, 35:702–714, 2007

ISSN: 0192-6233 print / 1533-1601 online
DOI: 10.1080/01926230701481915

Pulmonary Toxicity of Expancel® Microspheres in the Rat

DALE W. PORTER,[1] ANN F. HUBBS,[1] PAUL A. BARON,[2] LYNDELL L. MILLECCHIA,[1] MICHAEL G. WOLFARTH,[1] LORI A. BATTELLI,[1] DIANE E. SCHWEGLER-BERRY,[1] CHRISTOPHER M. BEIGHLEY,[1] MICHAEL E. ANDREW,[1] AND VINCENT CASTRANOVA[1]

National Institute for Occupational Safety and Health, [1]Health Effects Laboratory Division, Morgantown, West Virginia 26505 and [2]Division of Applied Research and Technology, Cincinnati, Ohio 45226

ABSTRACT

Expancel® microspheres are thermoplastic microspheres enclosing hydrocarbon. These microspheres expand when heated, producing many applications. Because they have unknown biological persistence and toxicity, we investigated the toxicity of two unexpanded (11.1 and 15.4 μm mean diameter) and two expanded (3.1 and 5.5 μm mass median aerodynamic diameter) Expancel® microspheres in intratracheally-instilled, male, Sprague–Dawley rats. Pulmonary histopathology was evaluated at 28 days postexposure. Bronchoalveolar lavage fluid was evaluated at days 1, 7, 14, and 28 days postexposure. Crystalline silica was the positive control. By histopathology, both unexpanded and expanded microspheres caused granulomatous bronchopneumonia characterized by macrophages and giants cells, suggesting a persistent foreign body response. Expanded, but not unexpanded microspheres, also caused eosinophilic bronchitis and bronchiolitis, mucous metaplasia of airways and organized granulomatous inflammation with associated fibrosis and frequent airway obstruction. In contrast, alveolar macrophage activation, polymorphonuclear leukocytes, LDH and albumin in bronchoalveolar laveage fluid were initially elevated but returned to near control levels at 28 days, and did not reflect the persistent granulomatous bronchopneumonia caused by Expancel® microspheres. These findings emphasize the importance of histopathology for evaluating pulmonary toxicity, suggest that Expancel® microspheres are a potential occupational hazard, and indicate a need for additional studies on their potential pulmonary toxicity.

[Supplementary materials are available for this article. Go to the publisher's online edition of *Toxicology Pathology* for the following free supplemental resources: motion within unexpected microspheres in H&E-stained lung (supplementary Figure 1); broncholar epithelium 28 days following exposure to 551 DE 20 microspheres (supplementary Figure 2); membrane ruffling and some instances of phagocytosis within the microspheres (supplementary Figure 3)]

Keywords. Microspheres; Lung; Bronchoalveolar Lavage; Pulmonary inflammation; Occupational respiratory disease; Granulomatous pneumonia.

INTRODUCTION

Expancel® microspheres are composed of a thermoplastic shell that encapsulates hydrocarbon. These microspheres are available in 2 basic forms, unexpanded and expanded. Expanded forms of these microspheres are produced by heating the product. When heated, hydrocarbon within the thermoplastic shell expands, and the thermoplastic shell softens, resulting in an increase in the volume of the microspheres. Many properties of Expancel® microsphere are discussed on the Expancel web site ⟨http://www.expancel.com⟩ but the detailed composition of these microspheres remains proprietary information.

Expancel® microspheres are being used in a number of industrial applications, such as anti-slip coatings, car underbody coatings, industrial non-woven textiles, auto body filler and marine and hobby putties, cable fillings, cultured marble, civil explosives, model making materials, sealants and synthetic wood. Properties attributed to the Expancel® microspheres at the website (http://www.expancel.com) indicate the useful functions of Expancel® microspheres for these applications including increased friction of anti-slip coatings; decreased weight of car underbody coatings, auto body fillers and putties; improved thickness of non-woven textiles; increased electrical insulation in cable fillings; increasing the resistance of cultured marble to thermal shock; and, in civil explosives, increased explosive sensitivity. The wide range of applications for these materials suggests that human exposures are occurring. However, there is an absence of published data regarding any possible adverse health outcomes resulting from exposure to these microspheres.

Because Expancel® microspheres are an inhalable size and are particles of low solubility, we hypothesized that these particles, like other poorly soluble particles, would cause an inflammatory reaction in the lung (Cullen et al., 2000). However, we had no additional data to address concerns about the toxicity of lung-deposited Expancel® microspheres, such as their potential persistence in the lung, the severity or type of inflammation they could induce, or duration of the

Address correspondence to: Dale W. Porter, Ph.D., M/S 2015, NIOSH, 1095 Willowdale Road, Morgantown, WV 26505. E-mail: DPorter@cdc.gov

Disclaimer: The findings and conclusions in this report are those of the authors and do not necessarily represent the views of the National Institute for Occupational Safety and Health.

The authors would like to acknowledge the generous gift of the Expancel® microspheres from Maf Ahmad, President and Technical Manager, Expancel Inc. We also would like to thank Dean Newcomer, Patsy Willard and Sherri Friend for their outstanding histotechnology support. This research was supported by DHHS/CDC/NIOSH intramural project # 49277148.

Abbreviations: IT, intratracheal; BAL, bronchoalveolar lavage; INSPEC, Inertial Spectrometer; PBS, Ca^{2+} and Mg^{2+}-free phosphate-buffered saline; AM, alveolar macrophage; PMN, polymorphonuclear leukocyte; LDH, lactate dehydrogenase; AM CL, alveolar macrophage chemiluminescence; NBF, neutral-buffered formalin; NO, nitric oxide; SEM, scanning electron microscopy; H&E, hematoxylin and eosin; EMEM, Eagle's Minimal Essential Medium.

inflammatory response. Thus, we conducted an *in vivo* toxicological study in rats using 4 different microspheres in order to assess their potential to persist in the lung and for altering pulmonary histopathology in a subchronic 28-day study. Bronchoalveolar lavage cytology, changes in macrophage activation, and biochemical changes were used as a standard method to evaluate the development and/or resolution of lung changes.

Materials and Methods

Particles. In this study, 2 unexpanded microspheres (551 DU 20 and 551 DU 40) and 2 expanded microspheres (551 DE 20 and 551 DE 40) were investigated (Expancel, Inc, Duluth, GA). To determine their size and potential to reach the deep lung, microspheres were mixed with water and were collected on 0.4 μm track etch filters. For each microsphere particle type, 200 particles were imaged and sized using a JEOL 6400 scanning electron microscope (SEM). Because the expanded microspheres (551 DE 20 and 551 DE 40) had unusually low densities, aerodynamic diameter was determined for these microspheres. Three different approaches were used to determine the best estimate of the aerodynamic size distribution of the airborne expanded microspheres. The diameter distributions of collected 551 DE 20 and 551 DE 40 microspheres were measured using SEM. The aerodynamic diameter was calculated using the formula $D_{ae} = D_p (\rho_p/\rho_0)^{1/2}$, where D_p is the particle physical diameter as measured using SEM, ρ_p is the density of the particle, ρ_0 is the reference density (same as water) (Baron et al., 2001).

The density of the particles was initially assumed to be that supplied by the manufacturer for each material. The Aerodynamic Particle Sizer (Model 3321, TSI, Inc. St. Paul, MN) is a real-time instrument that approximately measures aerodynamic diameter of particles in the range of 0.5 to 15 μm by accelerating them through a nozzle at high velocity and measuring their velocity (Baron and Willeke, 2001), and corrections are made to observed sizes for particle density (Wang and John, 1987). A third instrument used to observe the particle aerodynamic diameter of the microspheres was the Inertial Spectrometer (INSPEC) (Belosi and Prodi, 1984). This instrument provides a more direct measure of aerodynamic diameter, but requires additional microscopy for quantitative measurement. This instrument was only used as a qualitative indicator to compare with the calculated aerodynamic sizes from the other instruments.

The α-quartz (silica), used as a positive control in this study (MIN-U-SIL 5, U.S. Silica, Berkeley Springs, WV), had a mean particle diameter of 3.7 μm (Ding et al., 2001). Endotoxin was measured in a water extract of each microsphere particle type using the Kinetic-QCL LAL Testing Made Easy 192 Test Kit (BioWhittaker, Walkersville, MD). For silica particles, endotoxin, if present, was inactivated by heating samples to 160°C for 90 minutes.

Animals. The animals used in these experiments were male Sprague-Dawley [Hla:(SD) CVF] rats weighing 200-225 g obtained from Hilltop Lab Animals (Scottdale, PA). The protocol was reviewed and approved by the NIOSH Animal Care and Use Committee. The animals were housed in an AAALAC-accredited, specific pathogen-free, environmentally controlled, barrier facility. The rats were monitored by serology to be free of endogenous viral pathogens, *Mycoplasma pulmonis* and cilia-associated respiratory bacillus; by PCR to be free of *Helicobacter spp*; by culture to be free of common respiratory bacterial pathogens; and by histopathology and fecal examination to be free of parasites. Rats were housed one per cage in individually ventilated microisolator cages (Thoren Caging Systems, Inc., Hazleton, PA), which were provided HEPA-filtered air. Alpha-Dri virgin cellulose chips and hardwood Beta-chips were used as bedding. The rats were maintained on ProLaB RMH 3500 diet (PMI Nutrition Inc, Brentwood, MO) and tap water was provided ad libitum.

Experimental Design. Rats were exposed by intratracheal (IT) instillation of a 3.0 mg/100 g body weight dose of a particle in saline, or an equivalent volume of saline (vehicle control). For each particle type, bronchoalveolar lavage (BAL) fluid evaluation was selected for evaluating the time course of lung changes because it is generally useful in toxicology screening in the lung, changes are easily quantified, macrophage activation can provide insight into mechanisms of lung injury, and a slightly adapted procedure can be used in humans (Henderson et al., 1985; Lapp and Castranova, 1993). Four time points (1, 7, 14 and 28 days post-exposure) were selected to assess acute inflammation and its potential resolution in BAL (6–8 rats per exposure group at each timepoint). These BAL changes were compared with histopathologic changes in lung (7–8 rats per exposure group) and tracheobronchial lymph node (6–8 per exposure group) at 28 days postexposure.

The specific microspheres chosen for study were representative of 2 types of microspheres, unexpanded (551 DU 20 and 551 DU 40) and expanded (551 DE 20 and 551 DE 40). The dose of particles administered, 3.0 mg/100 g body weight, was chosen because other occupational dusts, and specifically silica (positive control), are known to cause pulmonary inflammation and fibrotic responses in rats at similar dosages by 28 days. In addition, this dose is relevant for worker exposures to "particles not otherwise regulated." The estimated lung burden for "particle not otherwise regulated" in a 45-year working lifetime at the OSHA permissible exposure limit is 57 mg/g lung (Hubbs et al., 2005). With an average rat lung weight of 1 gram, the exposure in these rats roughly represented 10 to 20% of the potential lung burden that could accumulate over a working lifetime in a person. Crystalline silica was used as a positive control because it is a cytotoxic, inflammatory, poorly-soluble, particle that causes chronic progressive pulmonary inflammation and pulmonary dysfunction under occupational and experimental conditions (Porter et al., 2004; Rimal et al., 2005). A time-lapse video microscopy experiment was conducted to investigate microsphere phagocytosis by alveolar macrophages (AM) at 3 hours after exposure to 551 DU 20.

Intratracheal Instillation. For IT instillations, rats were anesthetized with an intraperitoneal (i.p.) injection of 30–40 mg/kg body weight sodium methohexital (Brevital, Eli Lilly and Company, Indianapolis, IN) and were IT instilled using a 20-gauge 4-inch ball-tipped animal feeding needle. A 20 mg/ml suspension of each particle type was prepared in 0.9% sterile saline (Baxter, Deerfield, IL). Rats received a 3.0 mg/100 g body weight dose of a particle; an equivalent volume of saline was used for vehicle controls.

Bronchoalveolar Lavage (BAL) and Cell Differentials. BAL was conducted at 1, 7, 14, and 28 days post-IT exposure. Rats were euthanized with an i.p. injection of sodium pentobarbital (>100 mg/kg body weight) and exsanguinated by cutting the abdominal vena cava. Next, a tracheal cannula was inserted and BAL was performed through the cannula using Ca^{2+} and Mg^{2+}-free phosphate-buffered saline (PBS), pH 7.4, supplemented with 5.5 mM D-glucose. The first lavage (6 ml) was kept separate from the rest of the lavage fluid. Subsequent lavages used 8 ml of PBS until a total of 80 ml of lavage fluid was collected. BAL cells were isolated by centrifugation (650 × *g*, 5 minutes, 4°C). An aliquot of the acellular supernatant from the first BAL (BAL fluid) was decanted and transferred to tubes for analysis of lactate dehydrogenase (LDH) and albumin. BAL cells isolated from the first and subsequent lavages for the same rat were pooled after resuspension in HEPES-buffered medium (10 mM N-[2-hydroxyethylpiperazine-N′-2-ethanesulfonic acid], 145 mM NaCl, 5.0 mM KCl, 1.0 mM $CaCl_2$, 5.5 mM D-glucose; pH 7.4), centrifuged a second time (650 × *g*, 5 min, 4°C), and the supernatant decanted and discarded. The BAL cell pellet was then resuspended in HEPES-buffered medium and placed on ice.

To assess pulmonary inflammation, cell counts of AMs and polymorphonuclear leukocytes (PMNs) were obtained using a Coulter Multisizer II (Coulter Electronics, Hialeah, FL). Cytospin preparations of BAL cells were made using a cytocentrifuge (Shandon Elliot Cytocentrifuge, London), stained with modified Wright-Giemsa stain and cell differentials were determined by light microscopy.

BAL Fluid Albumin and Lactate Dehydrogenase. BAL fluid albumin concentrations were determined as an indicator of the integrity of the blood-pulmonary epithelial cell barrier using a commercial assay kit (Albumin BCG diagnostic kit, Sigma Chemical Company, St. Louis, MO). BAL fluid LDH activities were determined as a marker of cytotoxicity using a commercial assay kit (Roche Diagnostics Systems, Montclair, NJ). Both the BAL fluid albumin and LDH assays were conducted using a COBAS MIRA Plus (Roche Diagnostic Systems, Montclair, NJ).

Alveolar Macrophage Chemiluminescence. AM chemiluminescence (AM CL) was determined as an indicator of reactive oxygen and nitrogen species production by AMs as previously described by our laboratory (Porter et al., 2002b), except 1 mM 1400 W, which is an inhibitor of inducible nitric oxide synthase (Garvey et al., 1997), was substituted for L-NAME in the assay. All chemiluminescence measurements were made with an automated luminometer (Berthold Autolumat LB 953) at 390–620 nm for 15 minutes, and the integral of counts per minute versus time was calculated.

Scanning Electron Microscopy of BAL Cells. For SEM, aliquots of BAL cells 1 day after 551 DU 20 particle exposure were cultured on cover slips for 1 hour, then fixed in Karnovsky's fixative and postfixed in osmium tetroxide. The cells were dehydrated in an ethanol series, dried using hexamethyldisalizane as the final solution, and coated with gold/palladium. All samples were imaged on a JEOL 6400 scanning electron microscope.

Lung and Tracheobronchial Lymph Node Histopathology. Rats, separate from those used for BAL studies, were euthanized with an i.p. injection of sodium pentobarbital (>100 mg/kg body weight) and exsanguinated by cutting the abdominal vena cava at 28 days post-IT exposure. Lungs were airway perfused with 6 ml of 10% neutral-buffered formalin (NBF). The left lung lobes were trimmed the same day and processed overnight in an automated tissue processor, embedded in paraffin, sectioned at 5 μm, and the mid-sagittal section was stained with hematoxylin and eosin, Masson's trichrome, and Alcian blue/periodic acid-Schiff, pH 2.5 for microscopic evaluation. Semi-quantitative pathology scores were assigned for pneumonia, alveolar epithelial cell hypertrophy and hyperplasia, eosinophilic bronchiolitis, and lung fibrosis. The semi-quantitative pathology scores were the sum of the distribution (extent) and severity scores as previously described (Hubbs et al., 2002). Briefly, severity was scored as none—0, minimal—1, mild—2, moderate—3, marked—4, severe—5 and distribution was scored as none—0, focal—1, locally extensive—2, multifocal—3, multifocal and coalescent—4, and diffuse—5. Fibrosis was evaluated in trichrome-stained sections using the same scoring system to quantify excess fibrous tissue.

The tracheobronchial lymph node were collected, immersion-fixed in 10% NBF and routinely processed as described above. Semi-quantitative pathology scores severity and distribution were assigned for lymphoid hyperplasia and granulomatous lymphadenitis using the same system described for the lung. The semiquantitative assessment of eosinophil infiltrates were assigned scores from 1 to 5 (representing severity) since the eosinophil infiltrates appeared to represent drainage from sites of eosinophilic inflammation rather than lymphadenitis. Semi-quantitative scores from 1 to 5 were also assigned for mast cell infiltrates for comparison with eosinophil infiltrates.

Video Microscopy. H&E sections were examined with a 60x oil objective on an AX70 Olympus photomicroscope. A Sony DXC-9000 3CCD color video camera and SimplePCI software (Compix Inc., Imaging Systems, Cranberry Township, PA) were used to capture images at 5 frames/sec.

Time Lapse Microscopy. Rats received a 3.0 mg/100 g body weight dose of the 551 DU 20 by IT instillation as described above. At 3 hours postexposure, BAL cell isolation and counting was conducted as described here, except the cells were resuspended in Eagle's Minimal Essential Medium (EMEM). Aliquots of either 0.25×10^6 or 0.5×10^6 BAL cells in 2 ml EMEM were placed in a Lab-Tek® 2-well chambered coverglass system (Nalge Nunc International, Rochester, NY). The coverglass chambers were placed in a stage-mounted microincubator (37°C, 5% CO_2) enabling observation of the preparation for several hours. A Zeiss LSM 510 confocal microscope system with an Axiovert 200 microscope, 63× oil immersion lens and Argon laser, was used to capture DIC images. Time lapse movies were made of cells over 45–80 minute time periods, with images captured at 1 minute intervals.

Statistical Analyses. Three different statistical analyses were performed. First, different particle-induced effects were examined individually at each time point for the BAL endpoints. Specifically, for each time point (post-IT day), the effect of each microsphere type on each BAL endpoint was

assessed using one-way analysis of variance, with experiment used as a block effect. Pair-wise comparisons were performed between each particle type and silica (positive control) and saline (vehicle control) using Dunnett's method to adjust for multiple comparisons. Two-sided tests were used with significance set at $p \leq 0.05$.

Second, changes were determined across time for each exposure group. Specifically, for each exposure group, the effect of post-IT day on each BAL endpoint was assessed using 1-way analysis of variance, with experiment used as a block effect. Pair-wise comparisons were performed for each post-IT day using the Tukey-Kramer method to adjust for multiple comparisons. Two-sided tests were used with significance set at $p \leq 0.05$.

In all the above analyses, tests were performed for homogeneity of variances between each post-IT day. In cases of unequal variances, analyses accounted for the heterogeneous variances enabling efficient inferences to be made.

Lastly, because the histopathology data are on an ordinal scale, contrasts between experimental groups were performed using the Wilcoxon rank sum test. Asymptotic tests and accompanying p values can be sensitive to the presence of numerous ties in sample values. One way to overcome this problem is to report exact p-values. Thus, exact p values are reported here because some of these data were heavily tied. Fisher's exact test was used to perform comparisons for the one dichotomous histopathology variable, bronchiolar obstruction status. Two-sided tests were used with significance set at $p \leq 0.05$.

RESULTS

Particles. Microsphere particle sizes are presented in Table 1. The expanded forms of the microspheres (551 DE 20 and 551 DE 40) had the largest particle sizes. However, the aerodynamic size distribution of the airborne expanded microspheres was 3.1 μm for 551 DE 20 and 5.5 μm for 551 DE 40, with geometric standard deviations of 1.28 and 1.30, respectively. For all the microsphere particle types, endotoxin was below the limit of detection, i.e., <0.05 EU/ml.

BAL Cell Differentials. BAL AMs were significantly higher in rats exposed to 551 DE 20 and 551 DU 20 than in saline controls at day 7 post-exposure. In rats exposed 551 DU 20, BAL AM levels returned to control levels by 14 days postexposure. BAL AM numbers remained elevated in 551 DE 20—exposed rats relative to saline controls at 14 and 28 days but were less than the BAL AM numbers in the silica positive control at these timepoints (Figure 1A). Silica exposure caused a sustained increase in BAL AMs through 28 days postexposure.

TABLE 1.—Expancel particle sizing

Particle type	Particle Diameter (μm)[a]	Aerodynamic Diameter (μm)[b,c]
551 DE 20	16.3 ± 4.2	3.1 (1.28)
551 DE 40	31.5 ± 7.0	5.5 (1.30)
551 DU 20	11.1 ± 2.0	
551 DU 40	15.4 ± 2.9	

[a] Values represent mean ± SD (n = 200 particles) determined by SEM as described in the Materials and Methods.

[b] Values represent mean and geometric standard deviation (shown in parentheses) of determinations made using SEM, APS and INSPEC as described in the Materials and Methods.

[c] Aerodynamic diameter measurements were not done on 551 DU 20 and 551 DU 40 because they are approximately the density of the plastic used to make them. Consequently, the TEM size should be the same as the aerodynamic size.

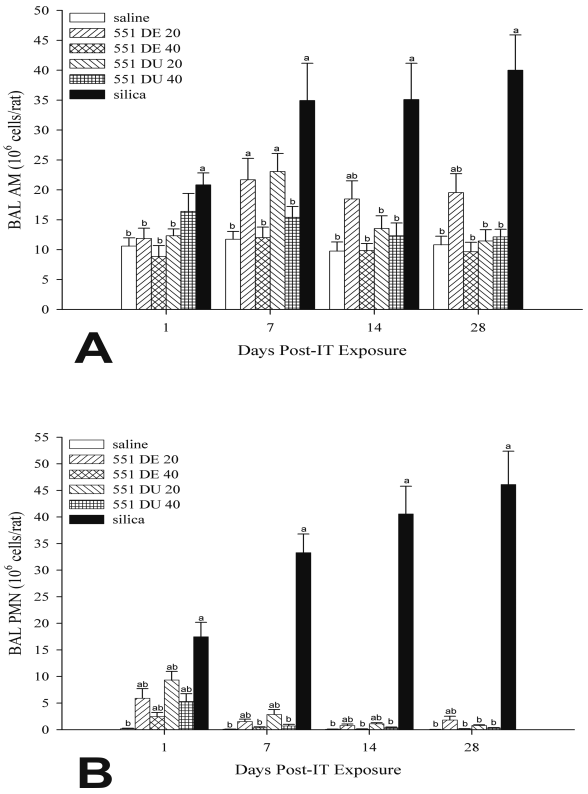

FIGURE 1.—Bronchoalveolar lavage alveolar macrophages and polymorphonuclear leukocytes. (A) Bronchoalveolar lavage macrophages and (B) polymorphonuclear leukocyte numbers were determined at 1, 7, 14, and 28 days post-IT exposure. For each post-IT exposure time, an "a" indicates a significant difference versus saline control group, and a "b" indicates a significant difference versus silica-exposed group. Values represent mean ± SE, n = 7–8 per group. Significance was set at $p \leq 0.05$.

In regards to BAL PMNs (Figure 1B), at 1 day postexposure, all microsphere-exposed groups were higher than the saline controls. However, in comparison to silica-exposed rats, saline- and microsphere-exposed rats had lower BAL PMNs at all post-exposure times examined, with this difference becoming greater with increasing exposure time. At 28 days post-IT, BAL PMNs from 551 DE 40 exposed, 551 DU 20 and 551 DU 40 exposed rats, had decreased from their 1 day post-IT values, and were not different from saline controls. For 551 DE 20 exposed rats, at 28 days post-IT, BAL PMNs remained significantly higher than saline controls. Silica exposure caused a sustained elevation of BAL PMNs throughout the 28-day time course, with an increase in PMNs on day 28 relative to day 1.

BAL Fluid Albumin and Lactate Dehydrogenase. BAL albumin was significantly elevated in all microsphere-exposed groups at 1 day post-exposure (Figure 2A). With the exception of 551 DE 20 exposed rats at 1 day post-IT, saline- and microsphere-exposed rats had significantly lower BAL fluid albumin levels at all postexposure times, in comparison to silica-exposed rats. At 28 days post-IT, BAL fluid albumin measured from 551 DE 20, 551 DE 40, and 551 DU 20 exposed rats had significant decreases in comparison to their 1

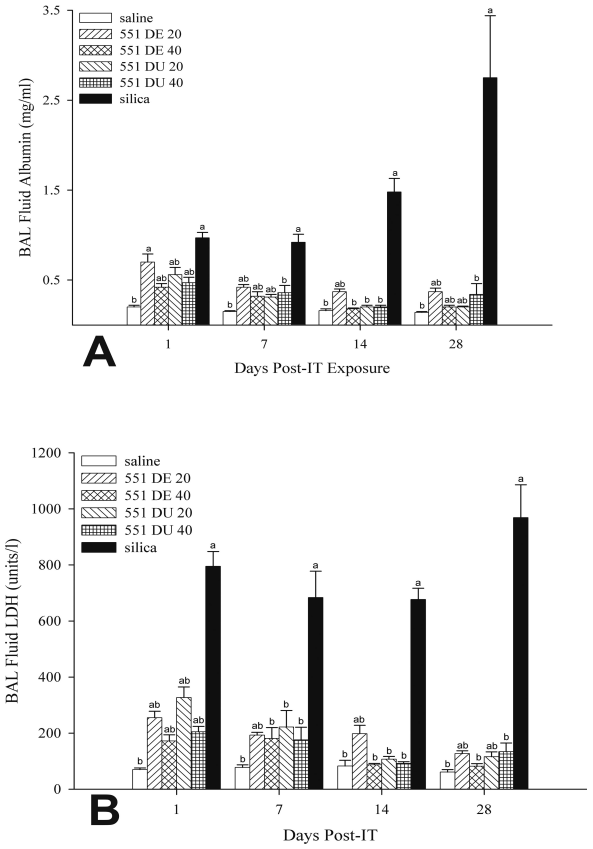

FIGURE 2.—Bronchoalveolar lavage fluid albumin and lactate dehydrogenase. (A) Bronchoalveolar lavage fluid albumin concentrations and (B) bronchoalveolar lavage fluid lactate dehydrogenase activities were determined at 1, 7, 14, and 28 days postexposure. For each postexposure time, an "a" indicates a significant difference versus saline control group, and a "b" indicates a significant difference versus silica-exposed group. Values represent mean ± SE, n = 7–8 per group. Significance was set at $p \leq 0.05$.

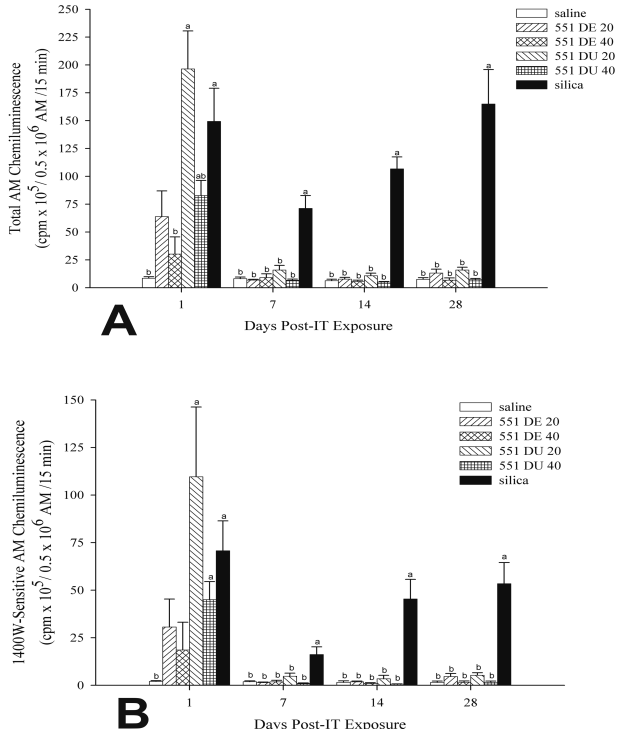

FIGURE 3.—Alveolar Macrophage Chemiluminescence. (A) Total alveolar macrophage chemiluminescence and (B) 1400W-sensitive alveolar macrophage chemiluminescence was determined at 1, 7, 14, and 28 days postexposure. For each postexposure time, an "a" indicates a significant difference versus saline control group, and a "b" indicates a significant difference versus silica-exposed group. Values represent mean ± SE, n = 7–8 per group. Significance was set at $p \leq 0.05$.

day post-IT values, but had still not completely returned to the saline control levels. Rats exposed to 551 DU 40 showed no significant decrease in BAL fluid albumin between 1 and 28 days post-IT exposure. For silica-exposed rats, at 28 days post-IT, BAL fluid albumin was 2.7-fold higher in comparison to 1 day post-IT exposure group, a change that was not significant.

BAL LDH was significantly elevated in all Expancel-exposed groups compared to control at 1 day post-IT (Figure 2B). In comparison to silica-exposed rats, saline- and microsphere-exposed rats had significantly lower BAL fluid LDH at all post-exposure times examined. At 28 days post-IT, BAL fluid LDH measured from 551 DE 20, 551 DE 40 and 551 DU 20 exposed rats had significant decreases in comparison to their 1 day post-IT values. However, the 551 DE 20 and 551 DU 20 exposed rats remained significantly higher than saline controls.

Alveolar Macrophage Chemiluminescence. Total zymosan-stimulated AM CL was increased at 1 day post-IT exposure by unexpanded microspheres (551 DU 20 and 551 DU 40) and silica (Figure 3A). In comparison to silica-exposed positive controls, total zymosan-stimulated AM CL in rats exposed to saline, 551 DE 40 and 551 DU 40 were significantly lower at 1 day post-IT exposure. At all subsequent time points, total zymosan-stimulated AM CL for rats exposed to either unexpanded or expanded microspheres were at saline control levels and less than the level in silica-exposed rats. In contrast, for silica-exposed rats, total zymosan-stimulated AM CL remained elevated at all time points.

1400W-sensitive zymosan-stimulated AM CL is the component of total zymosan-stimulated AM CL due to NO and NO-related reactions. In contrast to total zymosan-stimulated AM CL, the 1400W-sensitive zymosan-stimulated AM CL in rats 1 day after exposure to all 4 types of microspheres was indistinguishable from the response in silica. Similar to the total zymosan-stimulated AM CL response to unexpanded microspheres, at 1 day after exposure, unexpanded, but not expanded, microspheres caused a transient increase in 1400W-sensitive zymosan-stimulated AM CL. Thereafter, all Expancel® microsphere exposed groups had 1400W-sensitive zymosan-stimulated AM CL at saline control levels (Figure 3B). For silica-exposed rats, 1400W-sensitive zymosan-stimulated AM CL, as with total zymosan-stimulated AM CL, was elevated at all time points.

Scanning Electron Microscopy. BAL cells harvested from rats 1 day after exposure to 551 DU 20 microspheres have a highly ruffled surface (Figure 4), indicative of phagocytic cell activation.

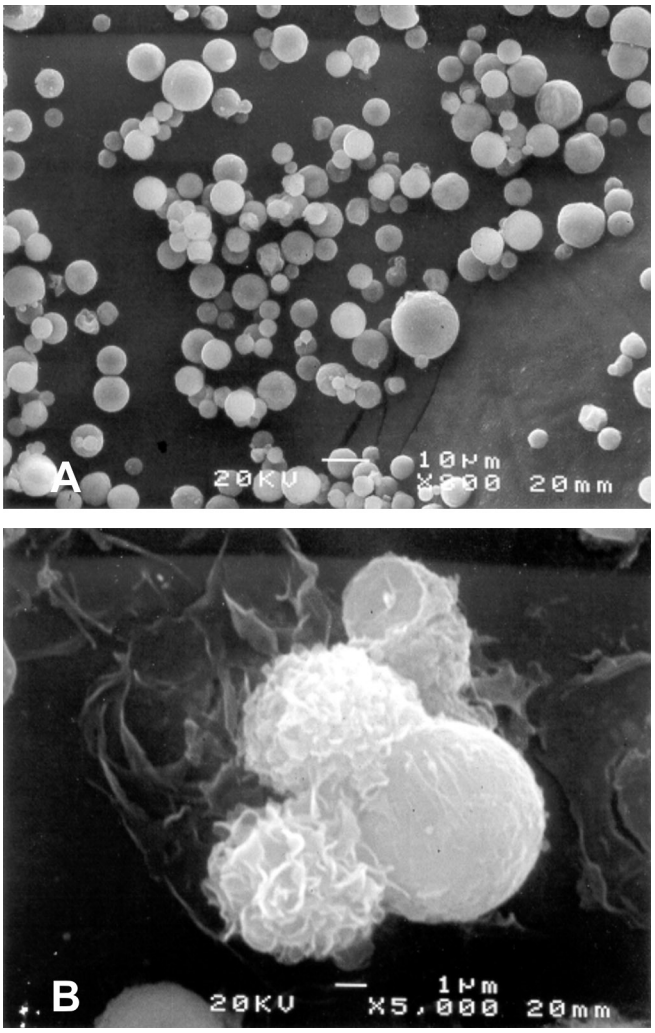

FIGURE 4.—Scanning electron microscope images. (A) 551 DU 20 microspheres as seen by scanning electron microscopy. (B) Phagocytes are clustered around a 551 DU 20 particle, and the phagocyte surfaces are highly ruffled, indicating cell activation in this scanning electron microscopy photomicrograph from a rat 1 day after exposure to 551 DU 20 microspheres.

Lung and Tracheobronchial Lymph Node Histopathology. Microspheres were easily visualized within the lungs of instilled rats. Unexpanded microspheres were seen as intracellular double-walled, particles. Within tissue, the size of both 551 DU 20 microspheres (Figure 5A) and 551 DU 40 microspheres (Figure 5B) varied. A unique feature of these unexpanded microspheres was their mobility in fixed tissue—as the slides warmed up, the inner portion of the unexpanded microspheres often moved with Brownian-like motion (Supplementary Figure 1). In addition to the double-walled microspheres larger, thin-walled, round structures; irregularly shaped thick-walled structures consistent with collapsed microspheres; faint round thin-walled structures; or intracytoplasmic spaces were also seen in the lungs of rats exposed to unexpanded microspheres. In tissue sections, expanded microspheres were thick-walled, irregularly round particles which accumulated transmitted light and were faintly birefringent with polarized light. There were fewer 551 DE 40 microspheres than 551 DE 20 observed in tissue. In addition, larger (>30 micron) intralesional spaces were frequently observed in rats exposed to both types of expanded microspheres (Figure 5C, Figure 5D). Some of these spaces contained foreign material consistent with remnants of a microsphere (Figure 5C).

At 28 days postexposure, all 4 types of microspheres and silica (the positive control) significantly increased pulmonary inflammation, characterized by large numbers of infiltrating macrophages but with some differences in the response. While lungs of rats with silicosis had multifocal to multifocal and coalescent alveolitis characterized by infiltrating macrophages and neutrophils which extended into peripheral alveoli and which rarely organized into discrete granulomas at 28 days (Figure 6A), the inflammatory response to all types of microspheres was characterized by macrophages, but fewer neutrophils, and consistently included giant cells. However, the type of microsphere particle affected the organization of the response and altered the contribution of eosinophils to the inflammatory response. The unexpanded microspheres, 551 DU 20 (Figure 6B, 6C) and 551 DU 40 (Figure 6D), consistently caused a macrophage and giant cell infiltrate without formation of discrete granulomas and without an eosinophil infiltrate.

While the response to unexpanded microspheres tended to center around bronchioles, the expanded microspheres, 551 DE 20 (Figure 6E, 6F) and 551 DE 40 (Figure 6G), consistently caused a more prominent bronchiolocentric distribution of inflammation, with frequent airway obstruction or obliteration, sometimes causing proliferative bronchiolitis obliterans and well-organized granulomatous inflammation. The expanded microspheres also caused eosinophilic bronchitis, bronchiolitis, and perivascular cuffing which was not seen in rats exposed to silica or unexpanded microspheres (Figure 6H, Table 2). While alveolar type II cells can be difficult to identify in paraffin sections, all types of microspheres and silica caused alveolar changes consistent with alveolar epithelial cell hypertrophy and hyperplasia (Table 2), with silica exhibiting a significantly greater effect than the microspheres. When all forms of particle-associated lung inflammation were combined, the scores for macrophage/giant cell infiltrates from the unexpanded microsphere were lower than those for silicosis (Table 2).

In trichrome-stained sections, expanded, but not the unexpanded microspheres, caused fibrosis in the foci of well-organized granulomatous pneumonia in all rats (Figures 7, 8, and 9). However, the mild to moderate fibrosis was generally restricted to these sites of well-organized granulomatous inflammation in the rats exposed to expanded microspheres, with alveolar septal fibrosis seen in only one rat exposed to expanded microspheres. Fibrosis was a consistent feature within foci of bronchiolar obstruction, including foci of proliferative bronchiolitis obliterans (Figures 8 and 9). In contrast, foci of fibrosis in the positive control, silica, extended beyond the rare foci of organized granulomatous inflammation and caused multifocal fibrosis of alveolar septa in all rats with a severity from minimal to moderate. Fibrosis scores for unexpanded microspheres were not different from saline controls and were significantly lower than silica and expanded microsphere groups (Table 2). The fibrosis scores for silica and expanded microspheres represent different sites of fibrosis within the lung.

TABLE 2.—Histopathology scores and incidence in the lung of rats exposed to Expancel® microspheres[a,b]

Histopathology Diagnosis	Particle Type					
	Saline (n = 8)	551 DU 20 (n = 8)	551 DU 40 (n = 8)	551 DE 20 (n = 7)	551 DE 40 (n = 7)	Silica (n = 8)
Eosiniphillic Bronchiolitis						
histopathology score	0.0 ± 0.0	0.0 ± 0.0	0.0 ± 0.0	4.6 ± 2.1*,†	5.7 ± 0.5*,†	0.0 ± 0.0
incidence	0/8	0/8	0/8	6/7	7/7	0/8
Alveolar Epithelial Hypertrophy and Hyperplasia						
histopathology score	0.00 ± 0.00	4.3 ± 1.8*,†	4.6 ± 1.9*,†	3.7 ± 2.6*,†	4.1 ± 1.9*,†	7.8 ± 0.50
incidence	0/8	7/8	7/8	5/7	6/7	8/8
Macrophage/Giant Cell Infiltrates[c]						
histopathology score	0.4 ± 1.1	4.9 ± 0.6*,†	5.5 ± 0.5*,†	7.4 ± 0.5*	6.3 ± 1.1*	7.1 ± 0.6
incidence	1/8	8/8	8/8	7/7	7/7	8/8
Lung Fibrosis						
histopathology score	0.0 ± 0.0	0.0 ± 0.0†	0.0 ± 0.0†	6.0 ± 0.0*,†	5.9 ± 0.4*	5.3 ± 0.7
incidence	0/8	0/8	0/8	7/7	7/7	8/8

[a] Values are means ± SE of the pathology scores for all rats in an experimental group.
[b] Values with an "*" indicates a significant difference from the saline control group, and values with a "†" indicates a significant difference from the silica-exposed group.
[c] The score for controls represents a single rat with a focus of mild alveolar histiocytosis and a focal minimal infiltrate of eosinophils and macrophages. Scores for Expancel®microsphere exposed rats represent macrophage and giant cell infiltrates and principally involved bronchioles and the peribronchiolar alveoli with formation of well-organized granulomas in rats exposed to expanded microspheres. Scores for silica-exposed rats represent alveolar infiltrates of macrophages and neutrophils with occasional granulomas or lymphogranulomas in some rats.

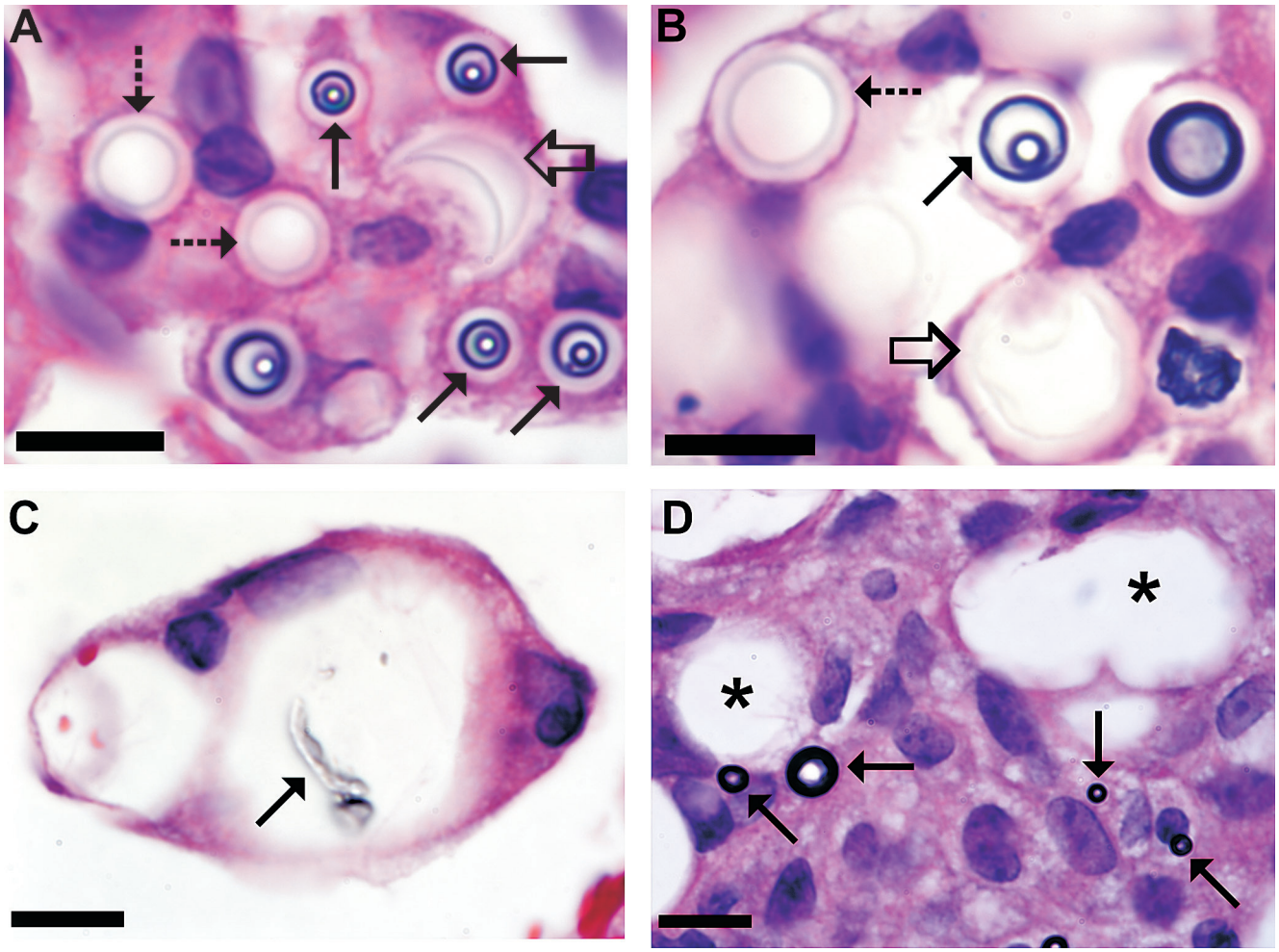

FIGURE 5.—Appearance of microspheres in tissue sections at 28 days postexposure. H&E stain. Bar = 10 μm. (A) 551 DU 20 microspheres in tissue sections were often double-walled particles (solid arrows). However, larger particles with thinner walls were also observed (dashed arrows), suggesting changes in microspheres with time. Occasional thin walled structures with unusual shapes (open arrow) were observed. (B) 551 DU 40 microspheres tended to be double-walled (solid arrow) but larger, thin-walled, round particles (dashed arrow) were also seen. Irregular shapes were occasionally seen in both thin (open arrow) and thick walled particles (to the right of the open arrow). (C) A giant cell contains 2 intracytoplasmic vacuoles in a rat instilled with 551 DE 40 microspheres. A remnant of foreign material presumed to be a degenerating microsphere is seen in the larger vacuole (solid arrow). (D) 551 DE 20 microspheres in tissue sections had a thick, single wall (solid arrows). Large intracytoplasmic spaces (asterisks) were also frequently observed.

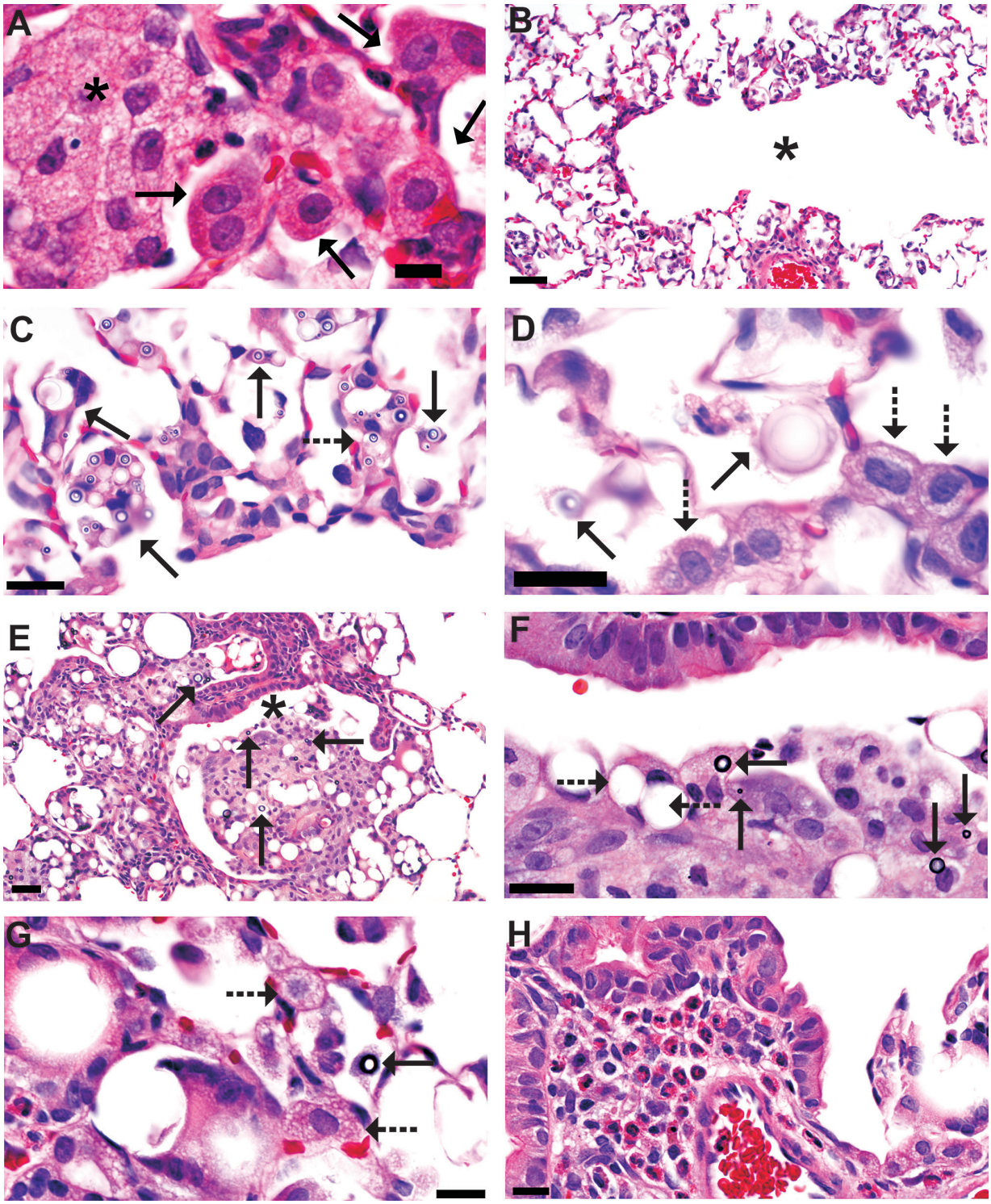

FIGURE 6.—Pulmonary response to silica particles and microspheres 28 days post-IT exposure. H&E stain. (A) Alveolar region of a rat exposed to silica. Large macrophage aggregates were frequently seen in alveolar spaces (*) and alveolar type II cells were hypertrophied and hyperplastic (solid arrows). Bar = 20 μm. (B) Lung of a rat exposed to 551 DU 20 demonstrating a cellular infiltrate in alveoli surrounding the alveolar duct. Bar = 50 μm. (C) A higher magnification from the lung of a rat exposed to 551 DU 20 microspheres shows microspheres of varying sizes within macrophages and multinucleated giant cells (solid arrows). Some microspheres appear to be in the interstitium (dashed arrow). Bar = 20 μm. (D) Lung of a rat exposed to 551 DU 40 microspheres showing variably sized microspheres (solid arrows) with associated hypertrophy and hyperplasia of alveolar epithelial cells (dashed arrow). Bar = 20 μm. (E) Lung of a rat exposed to 551 DE 20 microspheres showing granulomatous inflammation obstructing the opening of the terminal bronchiole into the alveolar duct (*) and extending into the adjacent alveoli. Microspheres (solid arrows) and many clear spaces are incorporated into the granulomatous response. Bar = 50 μm. (F) A higher magnification of the lung in E, showing macrophages extending into the lumen of the terminal bronchiole. Microspheres (solid arrows) were not always associated with cytoplasmic vacuoles (dashed arrows) and may be translocated during processing. Bar = 20 μm. (G) Lung of a rat exposed to 551 DE 40 microspheres showing a microsphere within an AM (solid arrow), giant cells with cytoplasmic vacuoles, histioctyic macrophages, and alveolar epithelial cell hypertrophy (dashed arrows). Bar = 20 μm. (H) Eosinophilic bronchiolitis in a rat exposed to 551 DE 40 microspheres. Bar = 20 μm.

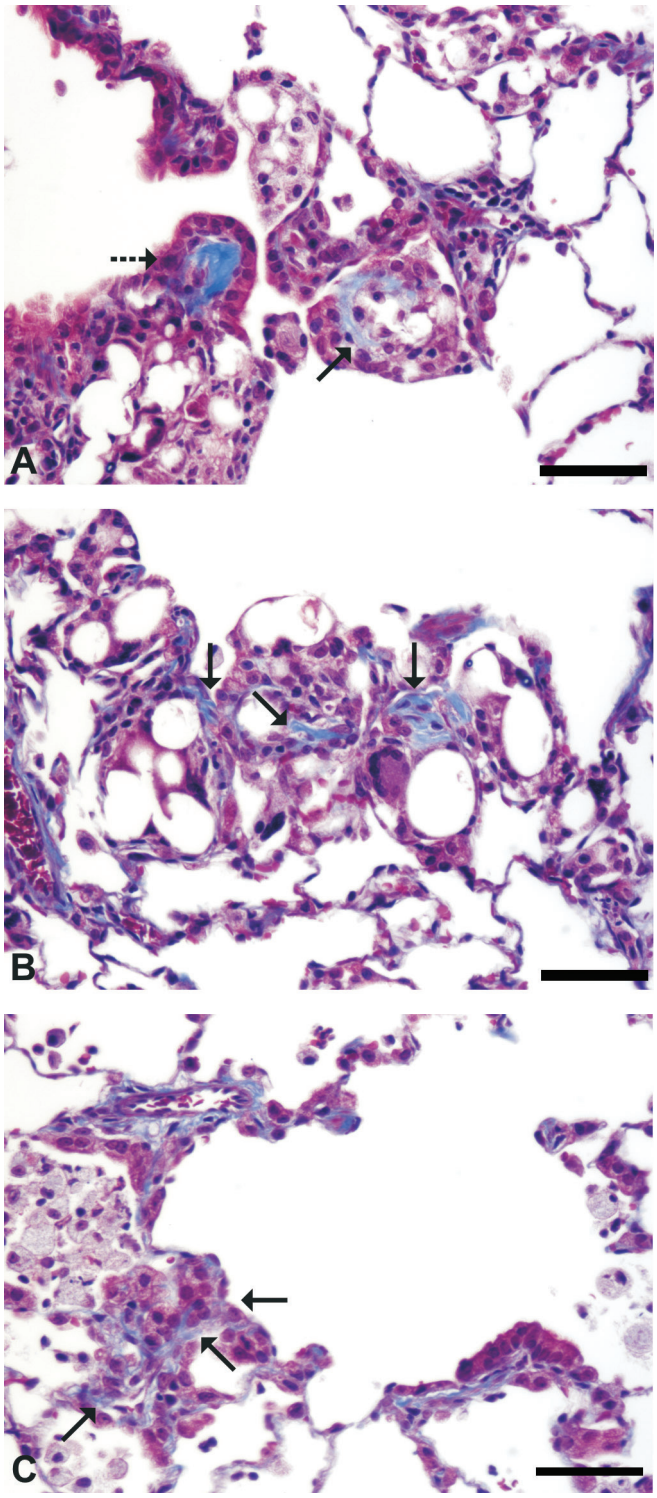

FIGURE 7.—Masson's trichrome-stained sections showing collagen deposition at 28 days after exposure (bar = 60 μm) (A) Collagen deposition (solid arrow) within granulomatous inflammation in the alveolar duct 28 days after exposure to 551 DE 20. The terminal bronchiole is constricted by fibrosis within the wall (dashed arrow). (B) Collagen deposition (solid arrows) within foci of granulomatous inflammation in the 1st generation alveolar duct from the terminal bronchiole 28 days after exposure to 551 DE 40. (C) Mild collagen deposition (solid arrows) in alveolar septa 28 days after silica exposure.

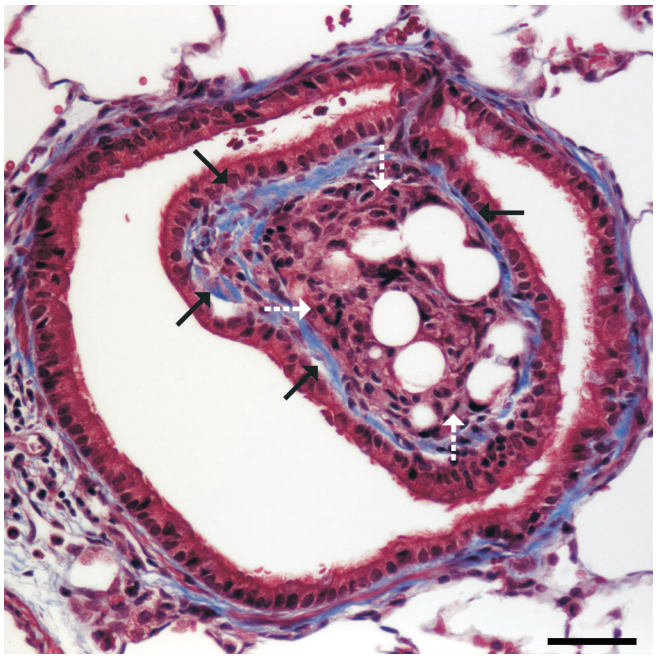

FIGURE 8.—A Masson's trichrome stained section of lung from a rat 28 days following 551 DE 40 exposure showing proliferative bronchiolitis obliterans containing well organized granulomatous inflammation (dashed arrows) and collagen deposition (solid arrows). Bar = 50 μm.

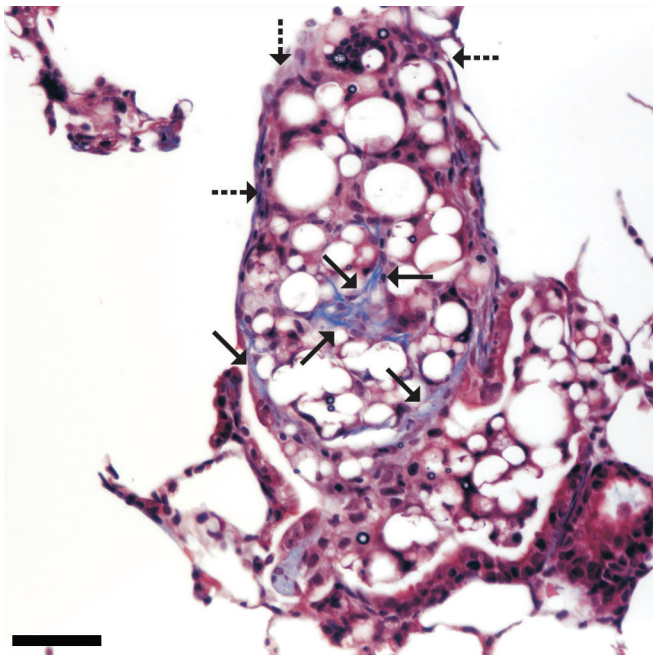

FIGURE 9.—A Masson's trichrome stained section from the lung of a rat 28 days following 551 DE 20 microsphere exposure. At the opening of the terminal bronchiole (dashed arrows) into the alveolar duct, a focus of well-organized granulomatous inflammation is partially lined by epithelium and contains irregular foci of collagen deposition as (solid arrows) indicated by blue staining. Bar = 50 μm.

TABLE 3.—Histopathology scores and incidence in the tracheobronchial lymph node of rats exposed to Expancel® microsheres

Histopathology Diagnosis	Particle Type					
	Saline (n = 8)	551 DU 20 (n = 8)	551 DU 40 (n = 8)	551 DE 20 (n = 7)	551 DE 40 (n = 7)	Silica (n = 8)
Lymphoid hyperplasia[b]						
histopathology score	0.00 ± 0.00†	0.00 ± 0.00†	0.00 ± 0.00†	0.00 ± 0.00†	0.00 ± 0.00†	9.38 ± 0.26*
incidence	0/6	0/8	0/8	0/6	0/7	8/8
Granulomatous lymphadenitis[b]						
histopathology score	0.00 ± 0.00†	0.00 ± 0.00†	0.00 ± 0.00†	0.00 ± 0.00†	0.00 ± 0.00†	6.00 ± 0.00*
incidence	0/6	0/8	0/8	0/6	0/7	8/8
Eosinophil accumulation[c]						
histopathology score	0.00 ± 0.00	0.00 ± 0.00	0.13 ± 0.13	0.43 ± 0.20	1.14 ± 0.51*,†	0.00 ± 0.00
incidence	0/6	0/8	1/8	2/6	4/7	0/8
Mast cell accumulation[c]						
histopathology score	0.00 ± 0.00	0.38 ± 0.38	0.25 ± 0.25	0.00 ± 0.00	0.43 ± 0.43	0.00 ± 0.00
incidence	0/6	1/8	1/8	0/6	1/7	0/8
Other	None	Expancel® microspheres were seen in 5 of the 8 lymph nodes.	None	Expancel® microspheres were seen in 3 of the 6 lymph nodes.	None	None

[a] Values are means ± SE of the pathology scores for all rats in an experimental group. Values with an "*" indicates a significant difference from the saline control group, and values with a "†" indicates a significant difference from the silica-exposed group.

[b] The pathology scores for lymphoid hyperplasia and granulomatous lymphadenitis represented the sum of the severity (scale of 0-5) and distribution (scale of 0-5) scores.

[c] Eosinophil accumulation was consistent with drainage from a site of eosinophilic inflammation within the lung, as opposed to eosinophilic lymphadenitis and severity but not distibribution was scored on a scale of 0-5. Mast cell accumulation was comparably scored for comparison with eosinophil accumulation.

In alcian blue-PAS stained sections (Supplementary Figure 2), the production of epithelial mucosubstances ranged from absent to minimal in control rats and in rats exposed to silica or unexpanded microspheres. In rats exposed to expanded microspheres, mild to moderate production of epithelial mucosubstances was observed in all but a single rat. In the rats exposed to expanded microspheres, the site of epithelial mucosubstance production involved airways of all sizes, from the mainstem bronchus to small bronchioles. Because mucous-producing cells are not normal in the bronchioles of rats, this was diagnosed as mucous metaplasia. The distribution of mucosubstance production in rats exposed to expanded microspheres was locally extensive to multifocal.

In tracheobronchial lymph nodes, 551 DU 20 and 551 DE 20 microspheres were demonstrated in 5 of 8 and 3 of 6 lymph nodes, respectively. Eosinophils were increased in lymph nodes from rats exposed to 551 DE 40 (Table 3).

Video Microscopy. Video microscopy captured the motion within the unexpanded microspheres in the H&E stained lung. This motion is demonstrated in Supplementary Figure 1.

Time-Lapse Microscopy. Both BAL dilutions provided numerous cells in the chambered preparation. Many of the BAL cells displayed one or more phagocytized microspheres; there were also some unphagocytized microspheres observed. Image captures at 1-second intervals revealed the Brownian-like movement within the microspheres. Image captures at 1-minute intervals, over 45–80 minute periods, revealed membrane ruffling and some instances of phagocytosis (Supplementary Figure 3). Although most of the microspheres were spherical, there were some distorted or crenulated shapes, suggesting changes to the microspheres after phagocytosis, although we were not able to detect the time course of these changes. At the end of the live cell observations, the cells were fixed and the nuclei were stained. Interestingly, the contents within the Expancel® microspheres in the fixed cells continued to exhibit the rapid Brownian-like motion observed in the H&E stained lung tissue sections.

DISCUSSION

Expancel® microspheres are particles without exposure standards. This means they fall into the broad category of "particulates not otherwise regulated," which includes many different solid particles (NIOSH, 2005). Thus, despite the many occupational uses for Expancel® microspheres, there is no published exposure or toxicity data available.

Initially, consideration was given as to whether the microspheres could penetrate into the lung airways. Based on microsphere sizing data (Table 1) and reported diameters of airways in rats (Kliment, 1973) and humans (Harris and Fraser, 1976), it is apparent that even the largest microsphere types can penetrate into the lung alveolar region. Furthermore, when the expanded microspheres' aerodynamic diameters were taken into consideration this appears to be even more likely, because the aerodynamic diameter values are much lower than the non-density-adjusted particle sizes and aerodynamic diameter is a major determinant of the ability to reach the deep lung. For the expanded microspheres used in these studies, the density corrected aerodynamic diameters of 3.1 μm and 5.1 μm represent sizes with high pulmonary deposition.

Depending upon the breathing pattern, particles with a diameter of 3 μm have alveolar deposition efficiencies of 15% to 36% and bronchial deposition efficiencies of 1% to 2% in nose-breathing humans (Heyder et al., 1986). Similarly, particles with a diameter of 5 μm have alveolar deposition efficiencies of 4% to 19% and bronchial deposition efficiencies of 2% to 5% in nose-breathing humans (Heyder et al., 1986). Indeed, the aerodynamic diameters of the expanded microspheres are similar to those of some particles intended for drug delivery to the lung (Cook et al., 2005; Usami et al., 2005). While particles in the size range for the unexpanded

microspheres (means of 11.1 and 15.4) have very low deposition efficiencies in the lungs of nose-breathing humans, mouth breathing is a common method of breathing in humans. Particles of 12 μm have alveolar deposition efficiencies of 0% to 2% and bronchial deposition efficiencies of 9% to 18% in mouth-breathing humans, depending upon the breathing pattern (Heyder et al., 1986).

Particles of 15 μm generally do not deposit in the alveoli, but have bronchial deposition efficiencies of 8% to 11% in mouth-breathing humans, depending upon the breathing pattern (Heyder et al., 1986). The 15 μm particle size is generally considered the upper size limit for significant pulmonary deposition in man (Snipes and Clem, 1981). However, particles larger than 5 μm have much lower pulmonary clearance than smaller particles. Indeed, only 14% of intratracheally instilled 15μm polystyrene microspheres are cleared from the lung with a half-time of 2.3 days and the remaining particles are apparently retained (Snipes and Clem, 1981). Thus, pulmonary deposition of the Expancel® microspheres would be expected in unprotected workers and clearance of the larger particles would predictably be low.

Currently there is considerable debate in the field of respiratory toxicology concerning the appropriateness of IT instillation versus inhalation exposure. However, a recent review by leading investigators in pulmonary toxicology indicated that IT instillations can be appropriately used in comparative pulmonary toxicology studies, such as those designed to compare the relative pulmonary toxicity of different particles (Driscoll et al., 2000). Thus, in this study, we used IT instillation as the exposure technique in order to compare the toxicity of 4 different types of microspheres.

Exposure to Expancel® microspheres caused several changes in BAL fluid at early timepoints. At 7 days post-IT, rats exposed to 551 DE 20 and 551 DU 20 showed significant increase in BAL AM relative to saline controls. In contrast, elevated BAL PMNs were seen in all microsphere-exposed rats in comparison to saline controls at 1 day postexposure. By 28 days post-IT, BAL PMNs in the 551 DE 20-exposed group remained elevated, the 551 DU 20-exposed group was only marginally increased, and PMN numbers were at saline control numbers in the remaining microsphere exposed groups. Similarly, BAL fluid LDH and albumin were significantly increased versus saline-exposed controls at 1 day post-IT, but decreased thereafter, approaching or returning to control levels by 28 days post-IT. At 1 day post-IT exposure 551 DU 20- and 551 DU 40-exposed rats had significant increase in AM CL, and these returned to saline-exposed control levels by 7 days post-IT. In general, BAL changes caused by Expancel® microspheres were less than the corresponding changes seen after an equivalent exposure to silica, the positive control. The BAL changes produced by silica were similar to those changes previously described in silica exposed rats, where BAL PMNs increased despite a decrease in lung silica burden, over time (Porter et al., 2004). Taken together, these data initially suggested that unequivocal pulmonary inflammation and damage had initially occurred after Expancel® microsphere exposure, but resolved after the initial period of inflammation.

Histopathologic examination of lung sections 28 days after microsphere exposure revealed that actual changes within the lung were far different from those suggested by BAL fluid analysis. Inflammation persisted at sites of microsphere deposition 28 days after exposure. In rats exposed to either unexpanded or expanded microspheres, the prominent giant cell response 28 days after exposure suggests an unresolved foreign-body type of reaction. The foreign-body granulomatous pneumonia is the expected response of the lung to persistence of the agent inciting the inflammatory response, i.e. the microspheres (William and Williams, 1983). By video confocal microscopy, unexpanded microspheres were readily phagocytized by BAL cells. In the first day after exposure, video confocal microscopy detected very little change in the unexpanded microspheres following phagocytosis. In the 28-day histopathology study, both the unexpanded and expanded microspheres persisted in the lung within phagocytic cells, explaining the persistent granulomatous inflammation.

In contrast to previous studies which have suggested that phagocytosis is not a mechanism for clearance of large respirable particles (Snipes and Clem, 1981), our study clearly demonstrates that Expancel® microspheres were present in macrophages and/or giant cells. However, translocation of Expancel microspheres to the tracheobronchial lymph nodes only occurred with, 551 DE 20 and 551 DE20, the smallest of the unexpanded and expanded microspheres, respectively. Thus, the larger Expancel microspheres do not translocated to the tracheobronchial lymph node, despite phagocytosis. The apparent degradation of some microspheres within phagolysosomes in our study is consistent with the conclusion of previous studies suggesting that large respirable particles are principally cleared from the lung by dissolution (Snipes and Clem, 1981). Additional studies of longer duration will be needed to determine how long the microspheres persist in the lung and whether or not the associated granulomatous inflammation persists, progresses or regresses with time.

Indeed, the time-dependent decrease in BAL LDH and albumin may actually reflect walling off of the inflammatory response so that LDH and albumin no longer leaked into the alveolar space that was sampled by BAL, although inflammation persisted. Similarly, time-dependent decreases in macrophage numbers, neutrophil numbers and macrophage activation in BAL fluid may reflect the organized granulomas caused by the expanded microspheres and the large size of the giant cells and macrophages in the alveolar spaces after unexpanded microsphere exposure. It is not surprising that the large activated macrophages and giant cells would fail to traverse the alveolar pores of Kohn or adhere to alveolar walls, causing their inefficient recovery in lavage fluid, resulting in the erroneous cytologic impression of recovery. Indeed, in rats exposed to respirable abrasive blasting agents, we have previously reported a discrepancy between BAL AMs and histopathologic alveolar inflammation which may result because activated AMs, such as those in an inflamed lung, are not as easily removed from the lung by BAL (Porter et al., 2002a). Previous researchers also noted that when airways were blocked by inflammation in toxicology studies, BAL changes did not reflect the extent of lung injury (Henderson et al., 1985). Similarly, the American Thoracic Society previously noted a lack of consensus among physicians regarding the usefulness of BAL in many interstitial lung diseases (Goldstein et al., 1990).

Despite the erroneous impression of recovery in the BAL fluid analysis, granulomatous inflammation clearly persisted and was demostrated by histopathology. Like other forms of inflammation, granulomatous inflammation can produce tissue damage and fibrosis (William and Williams, 1983). The additional observation of eosinophilic bronchitis, bronchiolitis and mucous metaplasia following 551 DE 20 and 551 DE 40 exposure, suggests that the response to the expanded microspheres involves more than simply a foreign-body response; this component of the response is reminiscent of the pulmonary response to allergens (Hogan et al., 2003). Since the expanded microspheres appeared to have thin outer walls after 28 days, this suggests particle changes with time in tissue. The hypothesis that substances released from the expanded microspheres could explain the more organized granulomatous inflammation, occasional foci of proliferative bronchiolitis obliterans, the eosinophilic bronchitis and bronchiolitis, and the mucous metaplasia which characterized the response to the expanded but not unexpanded microspheres.

Since recent evidence indicates that eosinophils are essential for the airway hyperresponsiveness, peribronchiolar fibrosis and smooth muscle hyperplasia of asthma (Humbles et al., 2004; Lee et al., 2004), the eosinophilic bronchiolitis suggests a need for future studies of pulmonary function in rats chronically exposed to expanded microspheres. Mucous metaplasia of airway epithelium is also associated with eosinophil infiltrates in some animal models of asthma (Lee et al., 2004), and mucous metaplasia was seen in the airways of rats exposed to expanded microspheres. In addition, the well-organized granulomas associated with expanded microspheres often obstructed airways and alveolar ducts while the development of early fibrosis within these lesions suggests a potential to persist and potentially affect lung function, supporting the need for pulmonary function studies in chronically exposed rats. The histopathologic changes seen in the lung and lymph node of rats exposed to the silica positive control were typical of the pulmonary changes previously described in rat models of silicosis (Porter et al., 2004). However, the giant cell response to unexpanded and expanded Expancel® microspheres and the eosinophilic bronchiolitis and mucous metaplasia in rats exposed to expanded microspheres are not seen in silicosis, suggesting fundamental differences between the response to silica and to Expancel® microspheres which need further study.

The histopathological results reported in this study suggest that these microspheres, particularly the expanded microspheres 551 DE 20 and 551 DE 40, may pose a pulmonary hazard. All of the Expancel® microspheres that we investigated histologically caused persistent bronchiolocentric inflammation. This places the inflammation at a critical site where air flow from conducting airways to and from alveoli may be impaired. The additional mucous metaplasia, eosinophilic bronchiolitis and the organized granulomas in rats exposed to 551 DE 20 and 551 DE 40, suggests a potential for airway obstruction. These findings suggest a need for follow-up studies which evaluate pulmonary function after exposure to Expancel® microspheres, to determine "no response" levels. Toxicological studies, which would include dose-response, chronic post-exposure time points, and biodurability determinations, are needed to more fully assess potential risk to workers.

References

Baron, P. A., Mazumder, M. K., and Cheng, Y.-S. (2001). Direct-reading techniques using particle motion and optical detection. In Aerosol Measurement: Principles, Techniques and Applications (P. A. Baron and K. Willeke, eds.), pp. 495–535. John Wiley & Sons, New York.

Baron, P. A., and Willeke, K. (2001). Aerosol fundamentals. In Aerosol Measurement: Principles, Techniques and Applications (P. A. Baron and K. Willeke, eds.), pp. 45–60. John Wiley & Sons, New York.

Belosi, F., and Prodi, V. (1984). Calculation of the deposition distance in the inertial spectrometer. *J Aerosol Sci* **15**, 381–4.

Cook, R. O., Pannu, R. K., and Kellaway, I. W. (2005). Novel sustained release microspheres for pulmonary drug delivery. *J Controlled Release* **104,** 79–90.

Cullen, R. T., Tran, C. L., Buchanan, D., Davis, J. M. G., Searl, A., and Jones, A. D. (2000). Inhalation of poorly soluble particles. 1. Differences in inflammatory response and clearance during exposure. *Inhal Toxicol* **12,** 1089–111.

Ding, M., Shi, X., Lu, Y., Huang, C., Leonard, S., Roberts, J., Antonini, J., Castranova, V., and Vallyathan, V. (2001). Induction of activator protein-1 through reactive oxygen species by crystalline silica in JB6 cells. *J Biol Chem* **276**, 9108–14.

Driscoll, K. E., Costa, D. L., Hatch, G., Henderson, R., Oberdorster, G., Salem, H., and Schlesinger, R. B. (2000). Intratracheal instillation as an exposure technique for the evaluation of respiratory tract toxicity: uses and limitations. *Toxicol Sci* **55**, 24–35.

Garvey, E. P., Oplinger, J. A., Furfine, E. S., Kiff, R. J., Laszlo, F., Whittle, B. J., and Knowles, R. G. (1997). 1400W is a slow, tight binding, and highly selective inhibitor of inducible nitric-oxide synthase in vitro and in vivo. *J Biol Chem* **272**, 4959–63.

Goldstein, R. A., Rohatgi, P. K., Bergofsky, E. H., Block, E. R., Daniele, R. P., Dantzker, D. R., Davis, G. S., Hunninghake, G. W., King, T. E., Jr., Metzger, W. J., et al. (1990). Clinical role of bronchoalveolar lavage in adults with pulmonary disease. *Am Rev Respir Dis* **142**, 481–6.

Harris, R. L., and Fraser, D. A. (1976). A model for deposition of fibers in the human respiratory system. *Am. Ind. Hyg. Assoc. J.*, 73–89.

Henderson, R. F., Benson, J. M., Hahn, F. F., Hobbs, C. H., Jones, R. K., Mauderly, J. L., McClellan, R. O., and Pickrell, J. A. (1985). New approaches for the evaluation of pulmonary toxicity: bronchoalveolar lavage fluid analysis. *Fundam Appl Toxicol* **5**, 451–8.

Heyder, J., Gebhart, J., Rudolf, G., Schiller, C. F., and Stahlhofen, W. (1986). Deposition of particles in the human respiratory tract in the size range 0.005–15 μm. *J Aerosol Sci* **17**, 811–25.

Hogan, M. B., Weissman, D. N., Hubbs, A. F., Gibson, L. F., Piktel, D., and Landreth, K. S. (2003). Regulation of eosionophilopoiesis in a murine model of asthma. *J Immunol* **171**, 2644–51.

Hubbs, A. F., Battelli, L. A., Goldsmith, W. T., Porter, D. W., Frazer, D., Friend, S., Schwegler-Berry, D., Mercer, R. R., Reynolds, J. S., Grote, A., Castranova, V., Kullman, G., Fedan, J. S., Dowdy, J., and Jones, W. G. (2002). Necrosis of nasal and airway epithelium in rats inhaling vapors of artificial butter flavoring. *Toxicol Appl Pharmacol* **185**, 128–35.

Humbles, A. A., Lloyd, C. M., McMillan, S. J., Friend, D. S., Xanthou, G., McKenna, E. E., Ghiran, S., Gerard, N.P., Yu, C., Orkin, S. H., and Gerard, C. (2004) A critical role for eosinophils in allergic airways remodeling. *Science* **305**, 1776–9.

Kliment, V. (1973). Similarity and dimensional analysis, evaluation of aerosol deposition in the lungs of laboratory animals and man. *Folia Morphologia* **21**, 59–64.

Lapp, N. L., and Castranova, V. (1993) How silicosis and coal workers' pneumoconiosis develop—a cellular assessment. *Occup Med* 8, 35–56.

Lee, J. J., Dimina, D., Macias, M. P., Ockur, S. I., McGarry, M. P., O'Neill, K. R., Protheroe, C., Pero, R., Nguyen, T., Cormier, S. A., Lenkiewicz, E., Colbert, D., Rinaldi, L., Ackerman, S. J., Irvin, C. G., and Lee, N. A. (2004). Defining a link with asthma in mice congenitally deficient in eosinophils. *Science* 305, 1773–1776.

NIOSH (2005). Particulates not otherwise regulated. In *NIOSH Pocket Guide to Chemical Hazards*. NIOSH Publication No. 2005-151.

Porter, D. W., Hubbs, A. F., Mercer, R., Robinson, V. A., Ramsey, D., McLaurin, J., Khan, A., Battelli, L., Brumbaugh, K., Teass, A., and Castranova, V. (2004). Progression of lung inflammation and damage in rats after cessation of silica inhalation. *Toxicol Sci* **79**, 370–80.

Porter, D. W., Hubbs, A. F., Robinson, V. A., Battelli, L. A., Greskevitch, M., Barger, M., Landsittel, D., Jones, W., and Castranova, V. (2002a). Comparative pulmonary toxicity of blasting sand and five substitute abrasive blasting agents. *J Toxicol Environ Health A* **65**, 1121–40.

Porter, D. W., Millecchia, L., Robinson, V. A., Hubbs, A., Willard, P., Pack, D., Ramsey, D., McLaurin, J., Khan, A., Landsittel, D., Teass, A., and Castranova, V. (2002b). Enhanced nitric oxide and reactive oxygen species production and damage after inhalation of silica. *Am J Physiol Lung Cell Mol Physiol* **283**, L485–93.

Rimal, B., Greenberg, A. K., and Rom, W. N. (2005) Basic pathogenetic mechanisms in silicosis: current understanding. *Curr Opin Pulm Med* **11,** 169–73.

Snipes, M. B., and Clem, M. F. (1981). Retention of microspheres in the rat lung after intratracheal instillation. *Environ Res* **24**, 33–41.

Usami, O. S., Biddiscombe, M. F., and Barnes, P. J. (2005) Regional lung deposition and bronchodilator response as a function of β-agonist particle size. *Am J Respir Crit Care Med* **172,** 1497–504.

Wang, H.-C., and John, W. (1987). Particle density correction for the aerodynamic particle sizer. *Aerosol Sci Technol* **6**, 191–8.

William, G. T., and Williams, W. J. (1983). Granulomatous inflammation–a review. *J Clin Pathol* **36**, 723–33.